that 0.5% of total trajectories starting from the Cl side lead to the HI product. This fraction, although not large, still amounts to a rough 10% of the total reactive events. The occurrence of this mechanism, not evidenced by Polanyi's calculations, is in agreement with the Walsh rule.[8] A IDT plot for this reactive mechanism is given in Figure 3. It shows how the HCl distance (shorter than that of the HI diatom in the initial part of the trajectory) becomes large after a few oscillations while the H atom binds to I.

(8) McDonald, J. D.; Le Breton, P. R.; Lee, Y. T.; Herschbach, D. R. *J. Chem. Phys.* **1972**, *56*, 769.

## Conclusions

A graphical analysis of the reaction path for the hydrogen atom colliding with the ICl molecule has shown that this system evolves through both a direct and a migratory path even for opposite geometries of attack. This fact implies that it is possible to obtain both hydrogen halide products irrespective of the angle of attack of the incoming atom (although the relative product fraction depends on it and on the electronegativity of the halogen atom). An obvious consequence of these results is the need for defining model reaction functions which have built in an angular-dependent branching weight.

**Registry No.** ICl, 7790-99-0; H atomic, 12385-13-6.

# Effects of Diatomic Reagent Alignment on the A + BC Reaction

**M. D. Pattengill,**

*Department of Chemistry, University of Kentucky, Lexington, Kentucky 40506*

**R. N. Zare,***

*Department of Chemistry, Stanford University, Stanford, California 94305*

**and R. L. Jaffe**

*NASA Ames Research Center, Moffett Field, California 94035* *(Received: February 25, 1987)*

Effects of diatomic reagent alignment on the prototype reaction A + BC → AB + C have been investigated by running classical trajectories on a modified version of the extended LEPS potential which permits the minimum energy path to be varied from collinear ($\theta_0$ = 180°) to broadside attack ($\theta_0$ = 90°). Preliminary model calculations are reported for the mass combination H + H′L → HH′ + L where H and H′ are heavy atoms and L is a light one. Two sets of empirical potential functions are chosen, one set for endothermic reactions (i.e., late barriers to reaction), the other set for exothermic reactions (i.e., early barriers). For each set, the minimum energy path is adjusted to be either $\theta_0$ = 90°, 135°, or 180° and the BC reagent diatomic is in either the ground vibrational state ($v$ = 0) or the first excited state ($v$ = 1). For corresponding $v$ = 0 and $v$ = 1 cases, the vibrational energy difference is ascribed to relative A,BC translational energy. For all cases, the initial BC rotational energies are chosen at random from a 300 K Boltzmann distribution. Thus, BC($v$=0) and BC($v$=1) collisions are chosen to have nearly equal total collision energies. Since the energetic characteristics of the minimum energy paths for each set of surfaces, corresponding to different values of $\theta_0$, are quite similar, the reported calculations permit direct investigation of the effects of varying minimum energy reaction path geometry on observed reaction attributes. Separate calculations have been performed for alignments in which the BC rotational angular momentum vector is either asymptotically parallel (or, equivalently, antiparallel) or asymptotically perpendicular to the direction of the initial relative A,BC velocity vector. For reaction on endothermic surfaces, a distinct effect [for both BC($v$=0) and BC($v$=1)] on the extent of product vibrational excitation is observed. Although the present studies are clearly model ones, the observed effect is in qualitative agreement with preliminary results obtained in alignment experiments on Sr + HF($v$=1). A similar but weaker effect is observed for BC($v$=0) on the exothermic surfaces but is absent for BC($v$=1). Beyond product energy disposals, the results obtained also demonstrate a marked effect, both for endothermic and exothermic potentials, of diatomic reagent alignment on reactive cross sections. Analysis of the observed trends suggests a possible underlying steric basis of the Polanyi rules which, for elementary bimolecular gas reactions, relate mode-specific excitation to extent of reactivity. In addition, the results obtained are suggestive of generalizations relating to the applicability of the Polanyi rules to reactions which favor noncollinear collisions.

## Introduction

Steric requirements on chemical reactivity have been inferred, for the most part, from indirect evidence. Examples are the need to include a steric factor in the hard-sphere model for calculating bimolecular rate constants[1,2] or the observation that one type of isomer predominates over another in the products of a reaction mixture.[3] Molecular beam studies under single collision conditions are beginning to provide the first direct measurements on the role of reagent approach geometry in controlling the outcome of a chemical reaction, a field which might be called reaction stereodynamics.[4] Here, reagents can be oriented by using external electric and magnetic fields or aligned by the absorption of plane-polarized light.[5] In spite of a few widely celebrated successes, experimental results are still sparse and the understanding of steric requirements remains presently at a primitive stage. [In accord with ref 4, by orientation of a molecule, we refer to the distribution of rotational angular momenta **J** which depends on

(1) Bunker, D. L. *Theory of Elementary Gas Reaction Rates*; Pergamon: Oxford, 1966.
(2) Smith, I. W. M. *Kinetics and Dynamics of Elementary Gas Reactions*; Butterworths: London, 1980.
(3) See: *Steric Effects in Organic Chemistry*; Newman, M. S., Ed.; Wiley: New York, 1956.
(4) Zare, R. N. *Ber. Bunsen-Ges. Phys. Chem.* **1982**, *86*, 422.
(5) *J. Phys. Chem.*, this issue and references cited therein.

0022-3654/87/2091-5489$01.50/0 

the sense of rotation, i.e., clockwise or counterclockwise; by alignment of a molecule, we refer to the anisotropic part of the J vector distribution which is independent of the sense of molecular rotation. Thus, if $\chi$ is the angle measured from the quantization axis to the J vector and the J vector distribution has cylindrical symmetry about this axis, then orientation involves the odd powers of cos $\chi$, i.e., the odd multipole moments, and alignment involves the even powers of cos $\chi$, i.e., the even multipole moments.]

We report here a computational study on the A + BC → AB + C bimolecular exchange reaction in which the BC diatomic is aligned with respect to the approach direction of atom A so that the initial rotational angular momentum vector of BC is either parallel (or, equivalently antiparallel) to or perpendicular to the initial velocity vector of A. The calculations are thus patterned after preliminary experiments[6] on the reaction Sr + HF($v$=1) → SrF + H in which the vibrationally excited hydrogen fluoride reagent is aligned by absorbing plane-polarized infrared light.

The calculations employ a modification of the extended LEPS potential[7] which permits the straightforward generation of noncollinear minimum energy reaction paths. In the studies reported, the minimum energy path was varied from purely collinear to purely broadside attack of A on BC. The scattering calculations, which consist of 3D classical trajectory studies, utilize a 300 K initial rotational energy distribution for BC. BC vibrational and A,BC relative translational energies are selected so that for a given potential surface and mass combination, the processes A + BC($v$=0) and A + BC($v$=1) are studied at essentially constant total collision energy. Small departures from constant total average energy result solely from the finite sampling of the BC rotational distribution. Additionally, it should be noted that the present calculations include contributions from BC molecules having zero rotational quantum numbers. These, of course, cannot be aligned in an experiment. However, since they constitute less than 4% of the total BC molecules for any given calculation, the effect of their presence should not be significant as regards conclusions relating alignment effects. However, their presence is beneficial when (vide infra) attempts are made to establish a connection between the cross sections computed here and fully orientation averaged cross sections. It should be noted that the present preliminary calculations are purely model ones not intended to mimic any specific experimental system. However, since they were inspired by the previously noted Sr + HF experiments, attention has been restricted herein to sample mass combinations of the class H + H'L → HH' + L where H and H' denote a heavy atom and L denotes a light one. In an attempt to gain a reliably complete picture of reagent diatomic alignment effects for this mass combination, calculations were performed on both endoergic and exoergic potential energy surfaces.

As will be discussed in detail below, results from the present model studies are in qualitative agreement with results obtained in the previously noted Sr + HF($v$=1) experiments. In particular, the calculations clearly demonstrate that diatomic reagent alignment can markedly affect the nature of reaction product energy partitionings. Probably more importantly, in the realm of the extent of reactivity, the computed results also demonstrate a clear effect of diatomic reagent alignment on reactive cross sections. An analysis of the cross-section results obtained provides insights into the applicability of the Polanyi rules[7,8] to reactions having noncollinear minimum energy reaction paths. These rules relate mode-specific reagent enhancement of reactivity to potential energy surface characteristics. Specifically, these rules state that at constant total collision energy, reagent vibrational excitation is preferable to relative reagent translational excitation in surmounting late potential barriers, which are typical of endothermic potential surfaces, and the reverse is the case for early barriers typical of exothermic potential surfaces. In addition to providing insights into the applicability of the Polanyi rules to reactions with noncollinear minimum energy reaction paths, the observed cross-section effects suggest that reagent alignment may play an important role in understanding the validity of the Polanyi rules. In the present calculations for collinear minimum energy reaction paths, mode-specific reactivity enhancement, expressed as the weighted sum of contributions from reagents aligned parallel and perpendicular, derives primarily from a single alignment component. For noncollinear minimum energy reaction paths, a similar contribution from a different alignment component of the diatomic is observed.

## Potential Energy Function

As noted above, the potential energy function employed is an augmented version of the extended LEPS potential originally proposed[7] by Polanyi and his co-workers. For A + BC, let $r_1$ denote the A–B bond distance, $r_2$ denote the B–C bond distance, $r_3$ denote the A–C bond distance, and $\theta$ denote the A–B–C angle; the A–B–C potential energy (relative to A + BC with BC at the bottom of its potential well) is then given by

$$V(r_1,r_2,r_3) = \frac{Q_1}{(1+S_1)} + \frac{Q_2}{(1+S_2)} + \frac{Q_3}{(1+S_3)} - \left[\frac{J_1^2}{(1+S_1)^2} + \frac{J_2^2}{(1+S_2)^2} + \frac{J_3^2}{(1+S_3)^2} - \frac{J_1J_2}{(1+S_1)(1+S_2)} - \frac{J_1J_3}{(1+S_1)(1+S_3)} - \frac{J_2J_3}{(1+S_2)(1+S_3)}\right]^{1/2} + A\{1-\exp[-\alpha(\cos\theta-\cos\theta_0)^2]\}\{T_1T_2+T_1T_3+T_2T_3\} \quad (1)$$

As usual, $(D_e)_i$, $\beta_i$, and $(r_e)_i$ represent Morse parameters of the diatom corresponding to subscript $i$. $(Q_i + J_i)/(1 + S_i)$ and $(Q_i - J_i)/(1 - S_i)$ are given, respectively, by the appropriate Morse and Sato–Morse[9] functions. For each diatom, $T_i$ is simply given by

$$T_i = (D_e)_i \exp\{-2\beta_i[r_i - (r_e)_i]\}$$

The quantities, $S_i$, $\theta_0$, $A$, and $\alpha$ are adjustable parameters which permit variation in the form of the A–B–C potential. In particular, the final additive term (missing in the normal extended LEPS function) permits the generation of noncollinear minimum energy reaction paths. For the present studies, the value of $\theta_0$ specifies the A–B–C angle which corresponds approximately to the minimum energy reaction path. It should be noted that since $\theta$ is the A–B–C angle, the potential form in eq 1 is unsuitable for cases in which BC is a homonuclear diatomic, and, because of the repulsive nature of the final cos $\theta$ containing term for small $\theta$, it is also unsuitable for cases in which BC is heteronuclear, but both ends of the molecule are reactive (i.e., AB + C and AC + B formation are both possible).

## Methodology

The augmented LEPS potential function described above was used to generate empirical model potential surfaces for the present study. By adjustment of the parameters $S_i$, $\theta_0$, $A$, and $\alpha$, two sets of potential surfaces were produced. For the first set of three potential surfaces, the A + BC → AB + C reaction is endoergic by 4.52 kcal/mol and the energetic barrier height to reaction which lies in the AB + C product channel is ca. 10 kcal/mol above the reactants asymptote. For the second set of three surfaces, A + BC → AB + C is exoergic by 4.52 kcal/mol and the energetic barrier to reaction which lies in the reactant A + BC channel is ca. 5 kcal/mol. Within each set the magnitude of the energy barrier to reaction and the shape of the minimum energy reaction path are quite similar, but the surfaces exhibit different preferred angles of attack of A on the BC bond axis corresponding to A–B–C bond angles of 90, 135, and 180°. Thus, for each set of surfaces, the minimum energy path for reaction spans the entire range from the end-on collinear approach of A to BC to the broadside attack of A on the BC bond axis.

Parameter values defining the six potential surfaces are presented in Table I. For both sets of potential functions, variations

(6) Karny, Z.; Estler, R. C.; Zare, R. N. *J. Chem. Phys.* **1978**, *69*, 5199.
(7) Kuntz, P. J.; Nemeth, E. M.; Polanyi, J. C.; Rosner, S. D.; Young, C. E. *J. Chem. Phys.* **1966**, *44*, 1168.
(8) Polanyi, J. C. *Acc. Chem. Res.* **1972**, *5*, 161.
(9) Sato, S. *J. Chem Phys.* **1955**, *23*, 592.

**TABLE I: Potential Parameters [Cf. Eq 1], As Noted in Text[a]**

| | | | |
|---|---|---|---|
| Endothermic Potentials | | | |
| $(D_e)_1 = 97.77$ | $\beta_1 = 0.9109$ | $(r_e)_1 = 2.7200$ | |
| $(D_e)_2 = 102.29$ | $\beta_2 = 1.898$ | $(r_e)_2 = 1.2740$ | |
| $(D_e)_3 = 41.97$ | $\beta_3 = 1.112$ | $(r_e)_3 = 2.2318$ | |
| $A = 0.4184$ | | $\alpha = 0.20$ | |
| $\theta_0 = 180$ | $S_1 = 0.12$ | $S_2 = 0.06$ | $S_3 = 0.12$ |
| $\theta_0 = 135$ | $S_1 = 0.12$ | $S_2 = 0.07$ | $S_3 = 0.12$ |
| $\theta_0 = 90$ | $S_1 = 0.24$ | $S_2 = 0.13$ | $S_3 = 0.24$ |
| Exothermic Potentials | | | |
| $(D_e)_1 = 102.29$ | $\beta_1 = 0.9109$ | $(r_e)_1 = 2.7200$ | |
| $(D_e)_2 = 97.77$ | $\beta_2 = 1.898$ | $(r_e)_2 = 1.2740$ | |
| $(D_e)_3 = 41.97$ | $\beta_3 = 1.112$ | $(r_e)_3 = 2.2318$ | |
| $A = 0.4184$ | | $\alpha = 0.20$ | |
| $\theta_0 = 180$ | $S_1 = 0.06$ | $S_2 = 0.12$ | $S_3 = 0.12$ |
| $\theta_0 = 135$ | $S_1 = 0.07$ | $S_2 = 0.12$ | $S_3 = 0.12$ |
| $\theta_0 = 90$ | $S_1 = 0.10$ | $S_2 = 0.20$ | $S_3 = 0.20$ |

[a] Subscript 1 denotes diatom AB, 2 diatom BC, and 3 diatom AC. Energies are given in kcal/mol, lengths in Å, and angles in degrees.

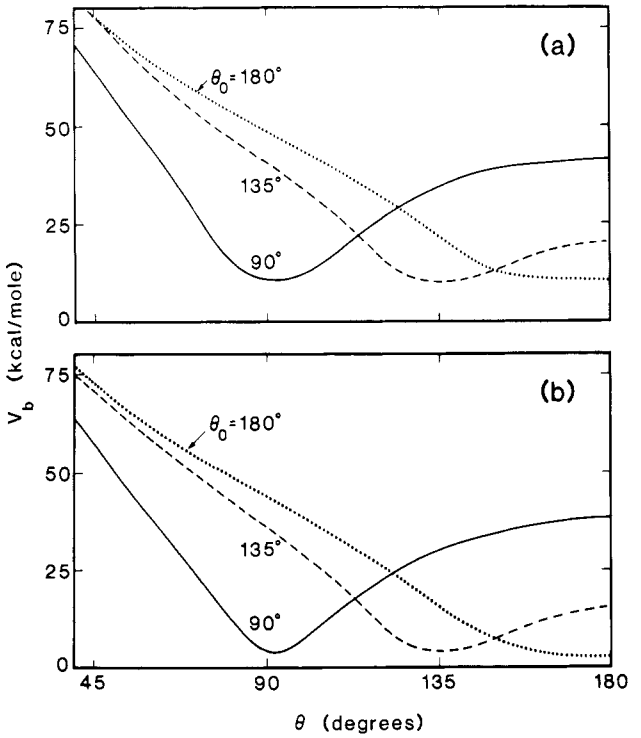


**Figure 1.** Plots of the minimum energy barrier to reaction vs. the A–B–C angle for potentials used in this study: (a) endothermic A + BC potential energy surfaces, and (b) exothermic A + BC potential energy surfaces. The value of $\theta_0$ identifies the A–B–C angle corresponding to the minimum energy path.

of the minimum energy barrier to reaction as a function of the A–B–C angle ($\theta$) are shown in Figure 1. Figure 2 presents energy contour maps of the minimum energy barrier reaction pathways (i.e., maps for $\theta_0$ = 90, 135, and 180°). The data appearing in Figure 1 were obtained by visual inspection of potential contour maps run at a resolution of 10° in $\theta$ and 0.1 Å in each of the bond distances A–B and B–C.

In an effort to recognize possible behavior specific to a particular H + H'L mass combination, the dynamics of six different mass combinations were investigated on each of the six potential surfaces employed in the study. Denoting a mass combination as ($m_A$, $m_B$, $m_C$) the specific mass combinations utilized were (with masses in amu): (80,80,1), (80,20,1), (40,80,1), (40,20,1), (20,80,1), and (20,20,1). Throughout the remainder of this paper and in the figures, these mass combinations are denoted (a) through (f), respectively. If asymptotic AB and BC vibrational zero-point energies are included, the endoergic surfaces are endothermic by 0.59–0.83 kcal/mol (depending on the mass combination) and the exoergic potentials are exothermic by 8.10–8.34 kcal/mol.

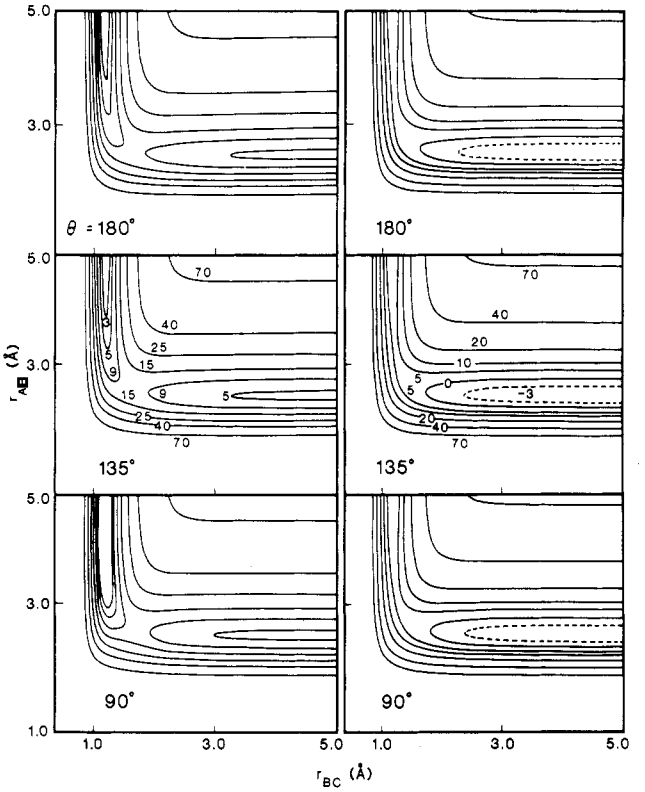


**Figure 2.** Contour plots of minimum energy paths for all potentials used in this study. Left panel of frames: endothermic surfaces; right panel of frames: exothermic surfaces. Energy values (in kcal/mol) corresponding to various contours are given in the middle frame of each panel.

The classical trajectory calculations were performed by techniques which have become standard.[10,11] For integration of Hamilton's equations of motion, a combined fourth-order Runge–Kutta–Gill,[11] sixth-order Gear hybrid integrator[12] algorithm was used. Trajectory integrations were performed with a program written specially for use on the NASA Ames Research Center's Cray X/MP computer. At a time step of $1.5 \times 10^{-16}$ s, individual trajectories typically required on the order of 0.1 s of CPU time. For each mass combination, potential surface, and initial BC vibrational state, roughly 2000 trajectories were computed.

For each potential surface and mass combination, the reactions A + BC($v$=0) → AB + C and A + BC($v$=1) → AB + C were studied at constant total translational plus vibrational energy. In all cases, initial BC rotational energies were chosen at random from a 300 K rigid rotor distribution. Initial relative translational plus BC vibrational energies were chosen so that with BC in the $v$ = 1 vibrational state the initial translational energy was slightly in excess of the minimum energy barrier for reaction. Depending on mass combination, total average collision energies were in the range 23.6–23.9 kcal/mol for endothermic potentials and in the range 18.0–18.3 kcal/mol for exothermic potentials.

As noted in the Introduction, the study was undertaken to investigate the effect of reagent alignment on reaction product attributes and cross sections. In keeping with experimental practice,[5,6] the reagent approach geometries considered where those in which the initial BC angular momentum vector is aligned either parallel (or, equivalently, antiparallel) or perpendicular to the initial A,BC relative velocity vector. The selection of these alignments is described in Figure 3. By use of standard proce-

(10) Truhlar, D. G.; Muckerman, J. T. In *Atom-Molecule Collision Theory-A Guide for the Experimentalist*; Bernstein, R. B., Ed.; Plenum: New York, 1979; Chapter 16.

(11) Pattengill, M. D. In *Atom-Molecule Collision Theory-A Guide for the Experimentalist*; Bernstein, R. B. Ed.; Plenum: New York, 1979; Chapter 10.

(12) Gear, C. W. *J. SIAM Numer. Anal., Ser. B* **1964**, *2*, 69.

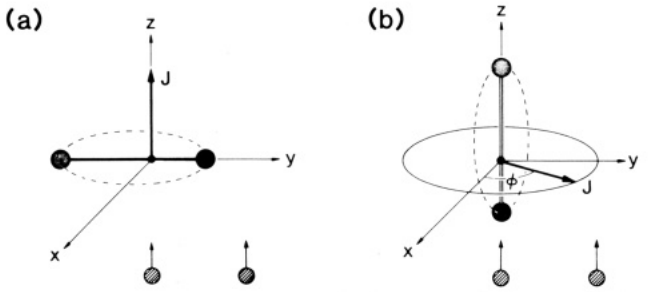


**Figure 3.** Schematic representations of (a) parallel and (b) perpendicular alignments. For each case, the diatom angular momentum vector lies parallel or perpendicular, as appropriate, to the A,BC relative velocity vector.

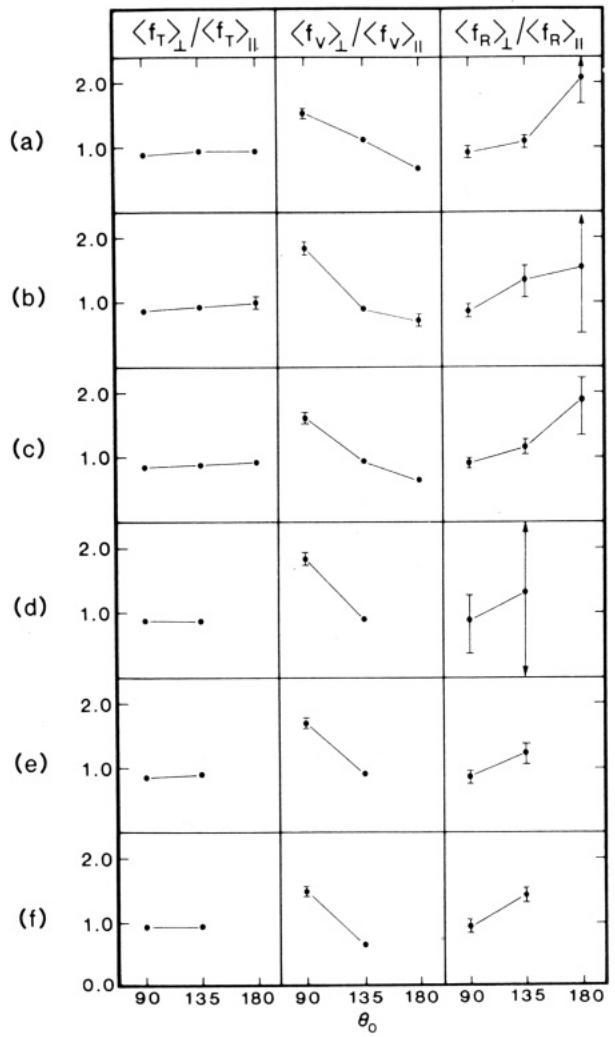


**Figure 4.** Ratios of product fractional translational $\langle f_T \rangle$, vibrational $\langle f_V \rangle$, and rotational $\langle f_R \rangle$ energy disposals, for each endothermic potential surface (characterized by a value of $\theta_0$). The results are for BC($v$=0) scattering. Plotted is the ratio of the component resulting from perpendicular alignment to the component for parallel alignment. For a definition of mass combinations corresponding to (a)–(f), see text. Where no error bars are indicated, they lie within the plotted data points.

dures,[10,11] the center of mass of BC is placed at the origin of a space-fixed right-handed coordinate system. Atom A is initially placed in the $Y,Z$ plane with the initial A,BC relative velocity directed along $+Z$. For such an arrangement, the A + BC collision impact parameter is simply given the value of the (positive) $Y$ coordinate of atom A.

For initial parallel BC alignment, BC executes rotation in the $X,Y$ plane with its angular momentum vector coincident with the $+Z$ axis. Initially placing A and BC far enough apart and randomly averaging over the value of the impact parameter produces

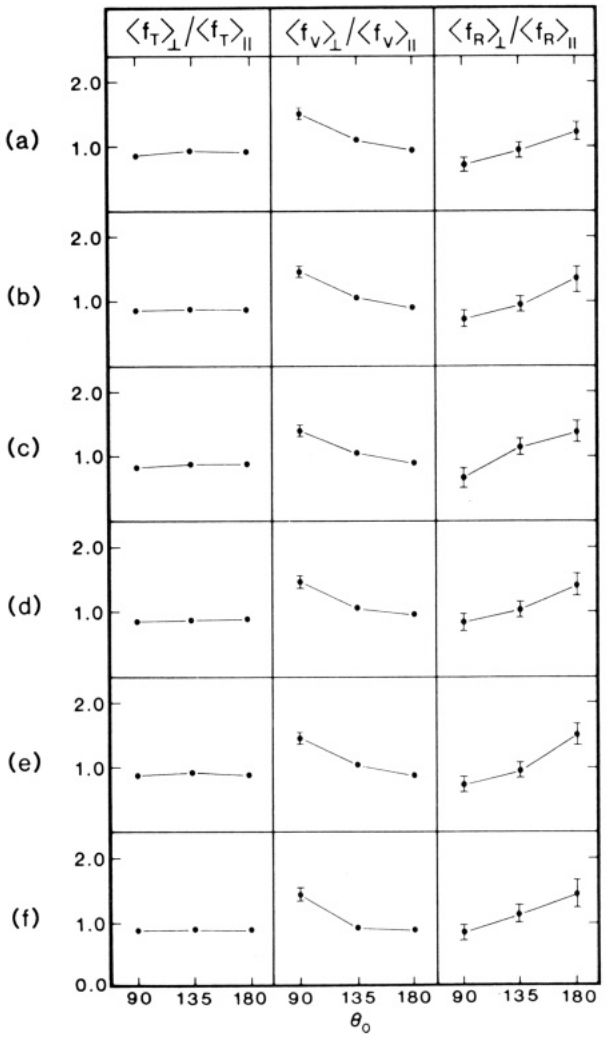


**Figure 5.** Same as Figure 4, but for BC($v$=1).

a random sampling of collisions with the initial BC angular momentum vector aligned parallel to the initial relative velocity vector. This situation is demonstrated in the left frame of Figure 3. For antiparallel alignment of the diatomic angular momentum vector with respect to the initial relative velocity vector, the sense of BC rotation is simply reversed from that described above and the angular momentum vector lies along the $-Z$ axis. For the present calculations the limiting cases of pure parallel and pure antiparallel alignment are equivalent. Thus, only the parallel case was investigated.

For initial perpendicular alignment of the BC rotational angular momentum vector with respect to the initial A,BC velocity vector, BC rotates in planes perpendicular to the $X,Y$ plane, and as shown in the right frame of Figure 3, its angular momentum vector is uniformly distributed in the $X,Y$ plane. For a BC angular momentum vector of magnitude **J**, its $X$ component is given by **J** sin $\phi$ and its $Y$ component is given by **J** cos $\phi$, where $\phi$ is uniformly distributed over the range 0 to $2\pi$ in the $X,Y$ plane. It should be noted that, in general, perpendicular alignment does not imply the existence of a coplanar, two-dimensional trajectory.

## Results and Discussion

As noted previously, a motivating consideration for the present calculations was the preliminary experimental observation[6] of a diatomic reagent alignment effect on vibrational energy disposal in the endothermic reaction Sr + HF. For HF($v$=1), it was found that perpendicular alignment of the HF angular momentum vector to the initial Sr atom velocity vector preferentially channeled reaction energy into product SrF vibration. On the basis of arguments derived from the Polanyi rules, it was suggested[6] that the origin of this effect was a noncollinear minimum energy

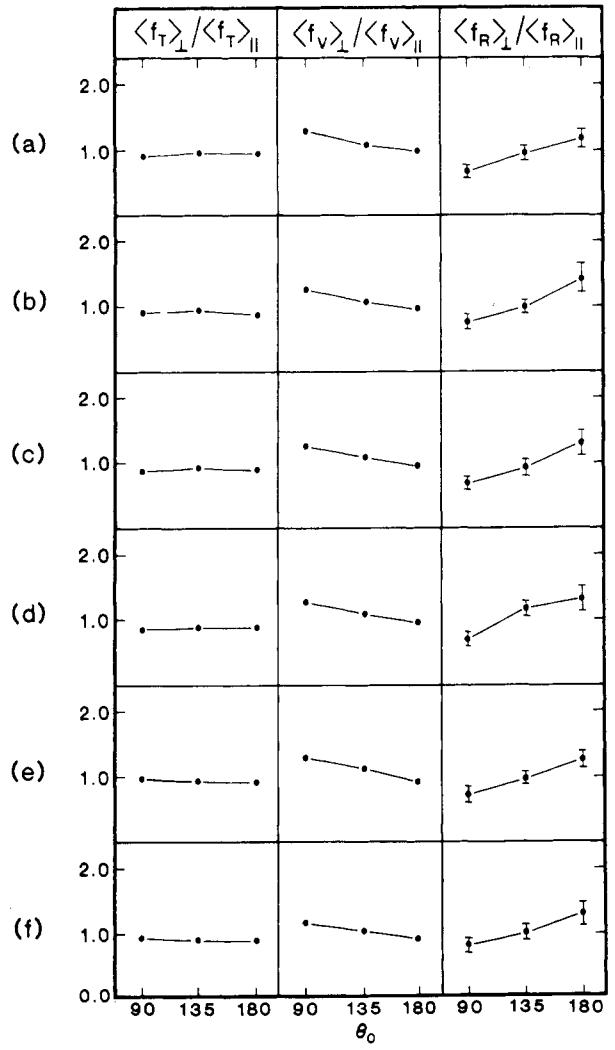


**Figure 6.** Same as Figure 4 but for BC($v$=0) on exothermic surfaces.

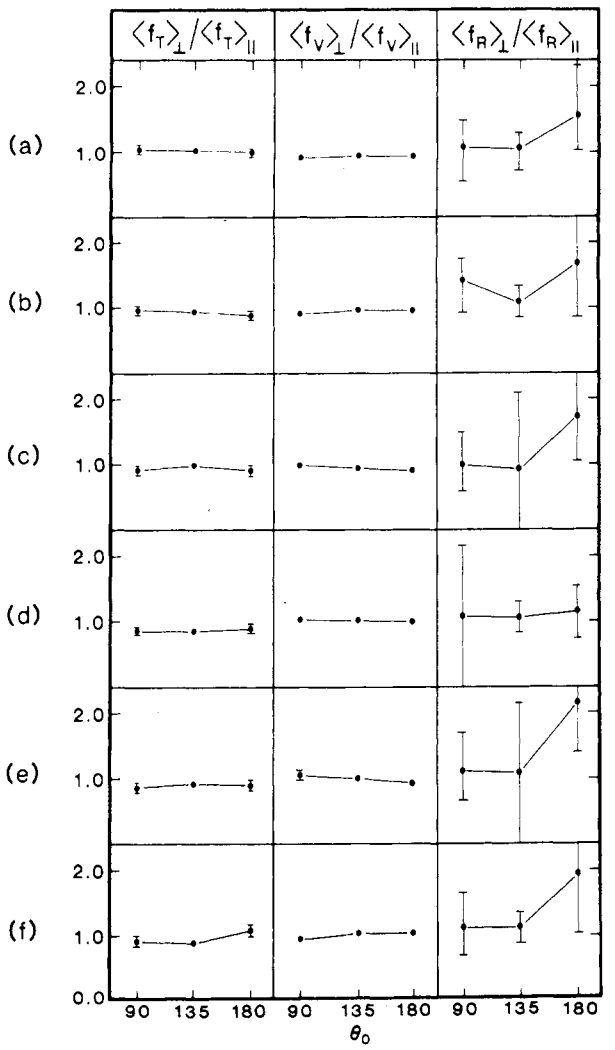


**Figure 7.** Same as Figure 4 but for BC($v$=1) on exothermic surfaces.

reaction path for Sr + HF → SrF + H. More recently, trajectory calculations[13] on an analytical fit to a high-quality Ca + HF ab initio potential function showed evidence of alignment effects on reactive cross sections. In the case of Ca + HF, the energetically preferred angle of attack of Ca on the HF bond was 75°—markedly noncollinear. By specifically investigating H + H′L dynamics on model potentials with and without preferred collinear reaction geometries, the present studies serve to address both the extent and the origin of the observed behavior.

To investigate effects associated with product energy disposal, for each potential surface set, mass combination, and BC initial vibrational state, we have computed for perpendicular and parallel orientations the fractions of available reaction energy entering product relative translation, vibration, and rotation. For compactness in presentation of the data, we have plotted ratios (perpendicular/parallel) of corresponding fractional energy disposals vs. values of $\theta_0$, the value of $\theta$ which characterizes the A–B–C angle corresponding to the minimum energy reaction path. These are presented in Figures 4–7.

For BC ($v$=0) on the endothermic surfaces (Figure 4), the results indicate virtually no preference for product translational excitation. This statement is true with regard to both preferred A + BC approach geometry and type of alignment. For product vibration and rotation there appears to be a trade-off with preferred broadside attack strongly favoring product vibrational excitation by perpendicular alignment and preferred collinear attack favoring product rotational excitation by perpendicular alignment. Because of the rather large error bars associated with the product rotation ratios, observed trends may be more apparent than real; however, the vibrational behaviors are clear and unambiguous.

Figure 5 presents data similar to that in Figure 4, except that results for BC($v$=1) on the endothermic surfaces are displayed. Qualitatively, the behavior is very similar to that observed for BC($v$=0), but somewhat less pronounced (especially with respect to vibration). It is gratifying to note that although they are purely model calculations, the endothermic BC($v$=1) product vibrational data are in qualitative agreement with the Sr + HF($v$=1) experimental data.[6]

Plots similar to those in Figures 4 and 5 are presented for the exothermic surfaces in Figures 6 and 7. For BC($v$=0), a slight set of trends reminiscent of those seen on the endothermic surfaces are evident. Excitation of BC to $v$ = 1 (cf. Figure 7) is, however, effective in removing any effects of either reagent approach geometry or diatomic reagent alignment on the product energy disposals. Further studies of H + H′L mass combinations on other model potential surfaces would be helpful in ascertaining whether or not the behavior observed here is a general characteristic of exothermic reactions involving the types of mass combinations considered.

Probably more important chemically than product energy disposals are the effects of alignment on the extent of reactivity, i.e., on reactive cross sections. While permitting generalizations on this aspect of reactivity, the results obtained in the course of this study also provide insights into the basis for the Polanyi rules[7,8] which relate mode-specific reactivity enhancement to potential energy surface characteristics. While these rules have been of paramount importance to the development of an intuitive un-

(13) Jaffe, R. L.; Pattengill, M. D.; Mascarello, F. G.; Zare, R. N. *J. Chem. Phys.* **1987**, *86*, 6150.

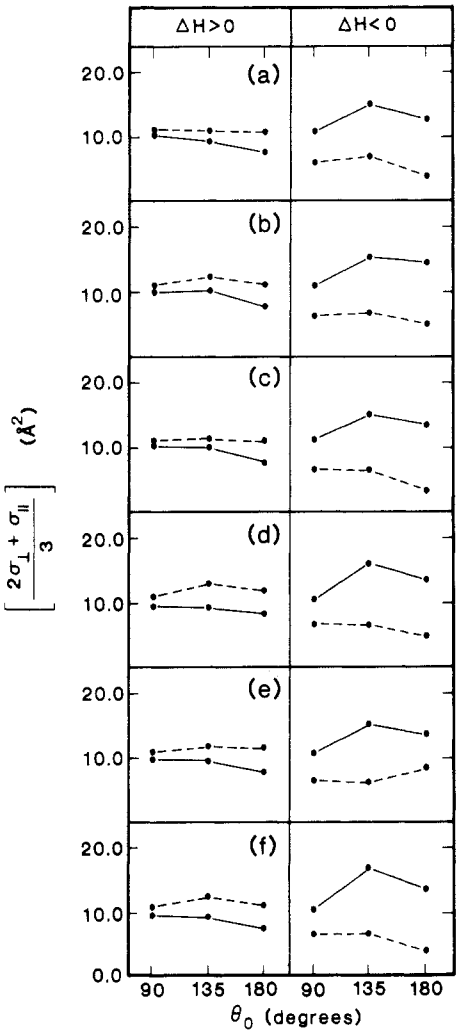


**Figure 8.** Estimated orientation-averaged reactive cross sections obtained (as described in text) by summing weighted contributions from aligned reactive cross sections. In each frame, solid curves correspond to A + BC($v$=0) scattering and dashed curves correspond to A + BC($v$=1) scattering. Left panel: results for various mass combinations on endothermic surfaces; right panel: results for various mass combinations on exothermic surfaces. For a definition of mass combinations corresponding to (a)–(f), see text. Plus or minus one standard deviations in the computed cross sections lies within the plotted points.

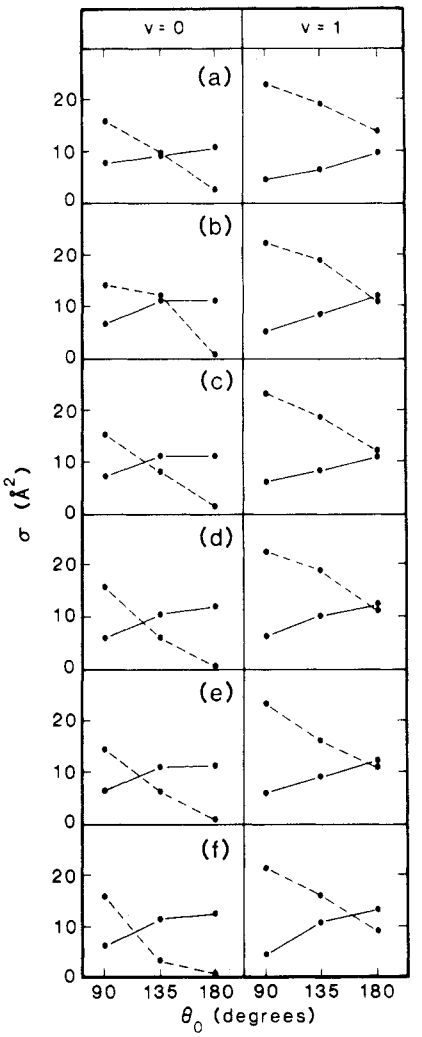


**Figure 9.** Perpendicular (solid lines) and parallel (dashed lines) reactive cross sections for various mass combinations on endothermic potentials characterized by the value of $\theta_0$. Left panel of frames: BC($v$=0); right panel of frames BC($v$=1). For a definition of mass combinations corresponding to (a)–(f), see text. Plus or minus one standard deviations in the computed cross sections lie within the plotted points.

derstanding of the dynamics of simple reactions, they were developed purely on the basis of investigation of reactions with preferred collinear reaction geometry.

The present results do not deal with fully orientation averaged cross sections. Nevertheless, it is reasonable to propose that the weighted sum of the cross sections obtained for the parallel and the two perpendicular initial reagent alignments should provide a reasonable approximation to the true orientation-averaged result. Invoking this premise, and weighting the perpendicular cross sections by $^2/_3$ and the parallel cross sections by $^1/_3$, Figure 8 presents plots of combined parallel and perpendicular cross sections vs. the A–B–C angle, $\theta_0$, which characterizes the geometry of the minimum energy reaction path. In each frame, the solid line represents the weighted sum of cross sections obtained for BC($v$=0) while the dashed line represents the weighted sum obtained for BC($v$=1). Recall that by design, regardless of the initial BC vibrational state, in each frame both curves correspond to the same total average collision energy.

For the endothermic potentials which have the reaction barrier in the exit channel (left panel of frames in Figure 8) the Polanyi rules assert that the reactive cross section should be enhanced by vibrational excitation of BC prior to reaction. In the context of the figure, this implies that the dashed curve should lie above the solid one in each frame. For preferred collinear reaction geometry, $\theta_0$ = 180°, the figure indicates convincingly that such behavior is the case. The interesting aspect of the endothermic portion of Figure 8 derives from the fact that as the preferred collision geometry approaches broadside attack, i.e., $\theta_0$ = 90°, the predicted dominance of BC($v$=1) weakens and for some mass combinations is essentially nonexistent.

For the exothermic potentials, which comprise the right-hand set of frames in Figure 8, the energy barrier to reaction is in the entrance channel. The Polanyi rules predict that reaction of A with BC($v$=0), which corresponds to higher relative translational energy, should be favored; i.e., the solid curve in each frame should lie above the dashed one. Again, the expected behavior is certainly observed for preferred collinear (as well as any other) reaction geometries. However, as was observed for the endothermic surfaces, the effect weakens (albeit, much less markedly than for the endothermic potentials) as the preferred broadside attack is approached.

Although the above commentary on the application of the Polanyi rules to noncollinear preferred reaction geometries is admittedly based on the premise that the weighted sum of cross sections for parallel and perpendicular alignments provides a reliable guide to the value of the orientation-averaged cross section, the observed trends are sufficiently marked to warn against indiscriminate application of the rules to (especially endothermic) reactions with significantly bent preferred reaction geometries.

Purely in the context of diatomic reagent alignment effects, the present results also demonstrate a marked effect of reagent

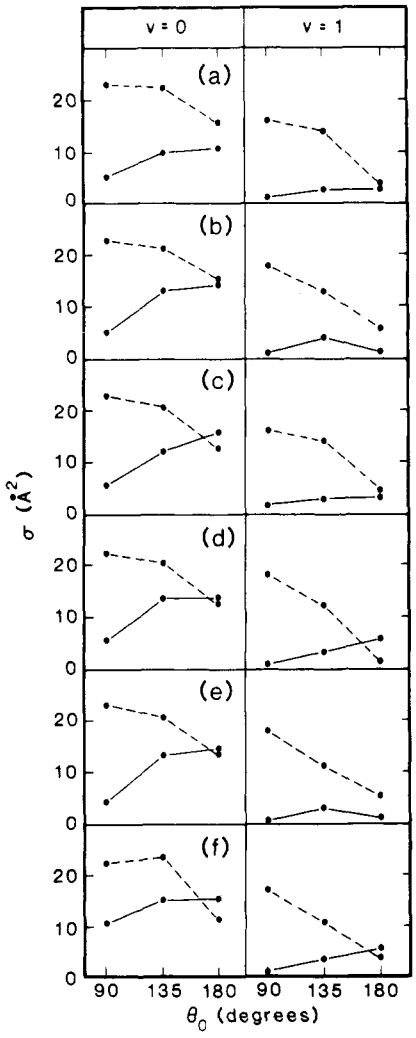


**Figure 10.** Same as Figure 9, but for exothermic surfaces.

alignment on reactive cross section. Figure 9 presents plots of parallel and perpendicular cross sections for the endothermic potentials and mass combinations studied. For these potentials at BC($v$=0), perpendicular alignments dominate the cross sections for $\theta_0$ = 180°, with the perpendicular and parallel curves reversing roles for preferred broadside attack ($\theta_0$ = 90°). For BC($v$=1), the parallel and perpendicular components are generally comparable for preferred collinear A + BC approach with the parallel component strongly dominating for pure broadside attack of A on BC. The interesting aspect, in particular for $\theta_0$ = 180°, is that the perpendicular alignment cross sections remain relatively constant on going from BC($v$=0) to BC($v$=1), while the parallel cross sections manifest large increases. Such behavior suggests that the change in contribution to the cross section from parallel aligned diatomic molecules is responsible for the increase in cross section in going from BC($v$=0) to BC($v$=1) on late barrier endothermic potential surfaces.

Figure 10 presents data similar to that in Figure 9 for the exothermic potential surfaces investigated. Here, the qualitative behavior of perpendicular alignment vs. parallel alignment cross sections is consistent for all mass combinations and for both BC vibrational states. While both components of the alignment cross sections generally increase (for all $\theta_0$ values), the $^2/_3$ weighting of the perpendicular component emphasizes its importance and suggests that enhancement in the perpendicular alignment component of the cross section plays some role in the predominance of relative translational energy in promoting overall reactivity on surfaces with early entrance channel barriers.

## Conclusion

The model studies reported herein, while limited to H + H′L → HH′ + L mass combinations, emphasize the information content contained in experiments utilizing aligned diatomic reagents. Alignment effects on product energy disposal and reaction cross section have been demonstrated. The dependence of these phenomena on potential surface characteristics has been explored. Beyond alignment effects themselves, the results also provide tantalizing evidence that the study of alignment effects may lead to a more complete understanding of the characteristics of fully orientation averaged cross sections. Future work will consider needed extensions to other classes of mass combinations and other potential surfaces.

*Acknowledgment.* M.D.P. expresses his thanks to the NASA Ames Research Center and R.N.Z. thanks the National Science Foundation NSF CHE 84-07270 for support. Both M.D.P. and R.N.Z. gratefully acknowledge the grant of computer time by NASA Ames.